Elsevier Editorial System(tm) for Atherosclerosis

Manuscript Draft

Manuscript Number:

Title: PCSK9 knock out mice are protected from neointimal formation in response to perivascular carotid collar placement

Article Type: Research paper

Section/Category: Basic Research

Keywords: PCSK9; smooth muscle cells; restenosis; small G proteins; cell proliferation; cell migration

Corresponding Author: Dr. nicola ferri,

Corresponding Author's Institution: University of MIlan

First Author: Nicola Ferri, PhD

Order of Authors: Nicola Ferri, PhD; Silvia Marchianò; Gianpaolo Tibolla; Roberta Baetta; Ashish Dhyani; Massimiliano Ruscica; Patrizia Uboldi; Alberico L Catapano; Alberto Corsini

Abstract: Proprotein convertase subtilisin kexin type 9 (PCSK9) is a key-regulator of hepatic low-density lipoprotein-receptor (LDLR). PCSK9 is expressed in cultured smooth muscle cells (SMCs) and co-localizes with SMCs in human carotid atherosclerotic plaques. The present study aimed at comparing the neointimal lesions induced by periadventitial carotid placement of a non-occlusive collar in PCSK9 knock-out (PCSK9-/-) and wild type (WT) littermate (PCSK9+/+) mice. Collared carotids of the PCSK9-/- mice showed less intimal thickening compared to WT mice ($p<0.05$), a decreased intimal media ratio ($p<0.02$) and tendency to higher lumen area. When compared with PCSK9-/-, carotid lesions of WT mice had a higher content of SMCs ($p<0.05$) and collagen ($p<0.05$). No difference in macrophage content was detected between the two groups. SMCs freshly isolated from PCSK9-/-, when compared to PCSK9+/+ cells, showed higher levels of the contractile markers α-smooth muscle actin (α-SMA; 2.24±0.36 fold; $p<0.01$) and myosin heavy chain II (MHC-II; 8.65±1.55 fold; $p<0.01$), and decreased levels of synthetic markers caldesmon (-54±14%; $p<0.01$). PCSK9-/- cells also showed in response to platelet-derived growth factor-BB (PDGF-BB) a slower proliferation rate, and impaired migratory capacity and G1/S progression of the cell cycle. The reconstitution of PCSK9 expression, by retroviral infection of PCSK9-/- SMCs, led to a downregulation of α-SMA (-56±2%; $p<0.01$) and significant induction of caldesmon (1.46±0.3 fold; $p<0.05$). Proliferation rate of SMCs PCSK9-/- was significantly lower compared to PCSK9 reconstituted cells. Taken together, the present results suggest that by sustaining SMC synthetic phenotype, proliferation and migration PCSK9 may play a pro-atherogenic role in the arterial wall.

Suggested Reviewers: Bodo Levkau
levkau@uni-essen.de
Dr. Levkau is an expert in vascular biology field

Elaine W Raines
ewraines@u.washington.edu
Dr. Raines discovered the PDGF and she has more than 30 years of experence in the atheroscleotic field

Bertrand Cariou
bertrand.cariou@univ-nantes.fr
Dr. Cariou works with the search group that discovered PCSK9.

paolo parini
paolo.parini@ki.se
Dr. Parini is an expert of lipid and cholesterol metabolsim field

Opposed Reviewers:

Graphical Abstract

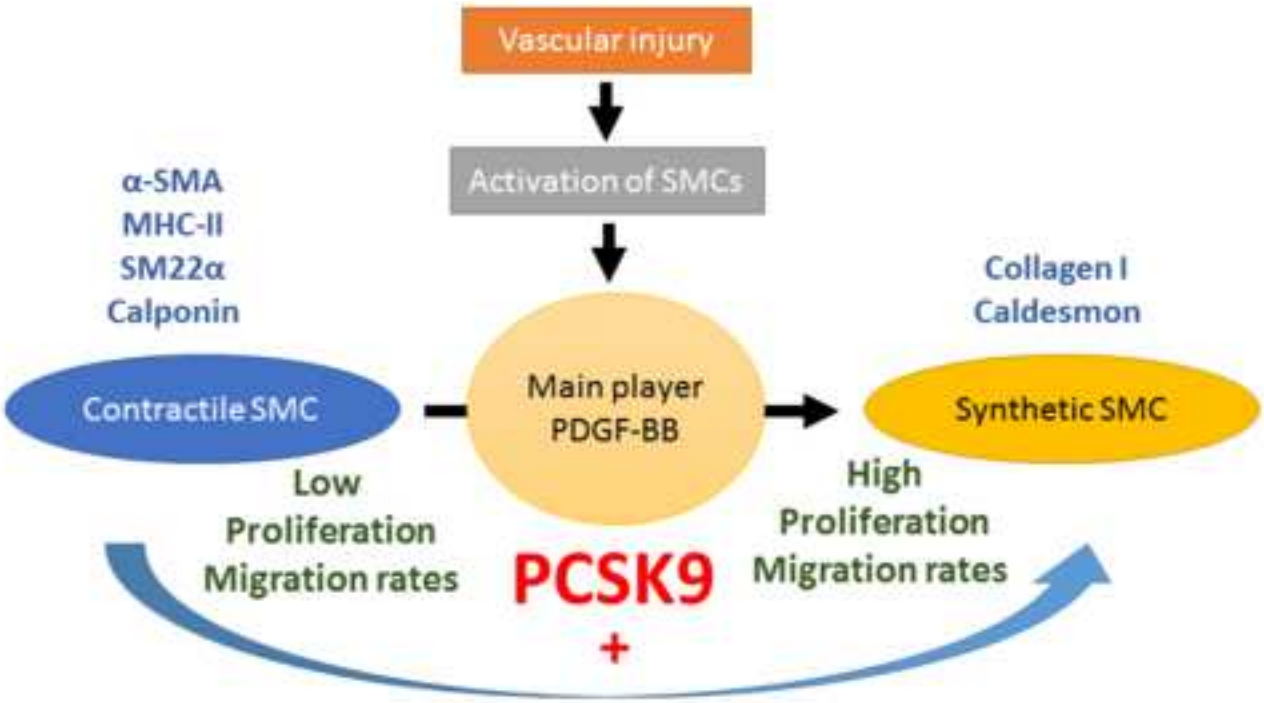

Highlights

In response to perivascular manipulation, the neointimal formation is reduced in PCSK9$^{-/-}$ mice

PCSK9 directly regulates smooth muscle cell differentiation, proliferation and migration

The reconstitution of PCSK9 expression in SMCs PCSK9$^{-/-}$ determines a switch towards a synthetic phenotype and rescue the impaired proliferation and migration capacities of SMCs PCSK9$^{-/-}$

SMCs PCSK9$^{-/-}$ respond less efficiently to the proliferative and chemotactic action of PDGF-BB

PCSK9 knock out mice are protected from neointimal formation in response to perivascular carotid collar placement

[1]Nicola Ferri, [2]Silvia Marchianò, [2,]Gianpaolo Tibolla, *[2]Roberta Baetta, [2]Ashish Dhyani, [2]Massimiliano Ruscica, [2]Patrizia Uboldi, [2,3]Alberico L. Catapano, and [2,3]Alberto Corsini.

[1]Dipartimento di Scienze del Farmaco, Università degli Studi di Padova, Padua, Italy; [2]Dipartimento di Scienze Farmacologiche e Biomolecolari, Università degli Studi di Milano, Milan, Italy; [3]Multimedica IRCCS, Milan, Italy.

* Present address: Monzino Cardiology Center IRCCS, Milan, ITALY, Italy.

Address correspondence to:

Nicola Ferri

Università degli Studi di Padova

Dip. Di Scienze del Farmaco

Largo Meneghetti 2, 35131, Padua, Italy

E-mail: nicola.ferri@unipd.it

Abstract

Proprotein convertase subtilisin kexin type 9 (PCSK9) is a key-regulator of hepatic low-density lipoprotein-receptor (LDLR). PCSK9 is expressed in cultured smooth muscle cells (SMCs) and co-localizes with SMCs in human carotid atherosclerotic plaques. The present study aimed at comparing the neointimal lesions induced by periadventitial carotid placement of a non-occlusive collar in PCSK9 knock-out ($PCSK9^{-/-}$) and wild type (WT) littermate ($PCSK9^{+/+}$) mice. Collared carotids of the $PCSK9^{-/-}$ mice showed less intimal thickening compared to WT mice ($p<0.05$), a decreased intimal media ratio ($p<0.02$) and tendency to higher lumen area. When compared with $PCSK9^{-/-}$, carotid lesions of WT mice had a higher content of SMCs ($p<0.05$) and collagen ($p<0.05$). No difference in macrophage content was detected between the two groups. SMCs freshly isolated from $PCSK9^{-/-}$, when compared to $PCSK9^{+/+}$ cells, showed higher levels of the contractile markers α-smooth muscle actin (α-SMA; 2.24±0.36 fold; $p<0.01$) and myosin heavy chain II (MHC-II; 8.65±1.55 fold; $p<0.01$), and decreased levels of synthetic markers caldesmon (-54±14%; $p<0.01$). $PCSK9^{-/-}$ cells also showed in response to platelet-derived growth factor-BB (PDGF-BB) a slower proliferation rate, and impaired migratory capacity and G1/S progression of the cell cycle. The reconstitution of PCSK9 expression, by retroviral infection of $PCSK9^{-/-}$ SMCs, led to a downregulation of α-SMA (-56±2%; $p<0.01$) and significant induction of caldesmon (1.46±0.3 fold; $p<0.05$). Proliferation rate of SMCs $PCSK9^{-/-}$ was significantly lower compared to PCSK9 reconstituted cells. Taken together, the present results suggest that by sustaining SMC synthetic phenotype, proliferation and migration PCSK9 may play a pro-atherogenic role in the arterial wall.

Introduction

Subendothelial accumulation of monocytes, lymphocytes, and some smooth muscle cell (SMC) progenitors from the blood and SMCs from the vessel wall, together with SMC-derived extracellular matrix (ECM), represent the prominent features of atherosclerotic plaques and restenosis after angioplasty [1-3].

Significant difference exists between intima and media SMCs, with the latter predominantly expressing proteins involved in the cell contraction, such as α-smooth muscle actin (SMA), myosin heavy chain II (MHC-II), calponin, and SM22-α; while those found in the intima have a higher migratory and proliferative index, and a greater synthetic capacity for extracellular matrix, proteases, and cytokines [4, 5].

A variety of atherogenic stimuli including extracellular matrix [6], cytokines, growth factors [7], shear stress [8], reactive oxygen species [9], and lipids [10] can facilitate the switch from "contractile" to "synthetic" phenotypic states. Once differentiated from "contractile" to "synthetic" phenotype, SMCs migrate and proliferate more readily and synthesize 25-30 times more collagen than contractile cells did [11]. In addition, they increase lipid synthesis [12] and express higher levels of very low density lipoproteins (VLDL), low density lipoproteins (LDL), and scavenger receptors allowing more efficient lipid uptake and foam cell formation [13].

Although a number of studies, conducted with genetically modified animals, have identified several signaling pathways or factors playing roles in SMC accumulation in the neointima, the mechanisms controlling SMC phenotypic switch are still not completely understood.

Proprotein convertase subtilisin kexin type 9 (PCSK9) represents the newest pharmacological target for controlling the hypercholesterolemia and, two monoclonal antibodies with PCSK9 inhibitory activity have been recently approved for clinical use [14, 15]. PCSK9 is mainly

synthesized by the liver, kidney and intestine, although other tissues and cell types express significant levels of PCSK9 [16]. In particular, we have previously reported that SMCs express PCSK9 *in vitro*, and that PCSK9 is detectable in human atherosclerotic plaque in regions occupied by SMCs [17]. Our observation was then confirmed by Perisic et al, showing that significant levels of PCSK9 mRNA are present in human carotid plaques and that these levels are upregulated, although not significantly, in comparison with control iliac arteries [18].

While it is clear that PCSK9 is expressed in SMCs in the atherosclerotic plaque; its role on SMCs biology is still elusive. In the present study, we have investigated the potential role of PCSK9 on SMC accumulation in neointimal lesions induced by perivascular carotid collar placement. This particular model was chosen since the vascular response that is observed after collar positioning in mice fed normal chow diet is mainly driven by SMC proliferation and migration processes, with minimal inflammation and, more importantly, the lesion size is independent from plasma cholesterol levels [19]. Our data indicate that in vivo the absence of PCSK9 confers a partial protection from neointimal formation. Furthermore in vitro PCSK9 positively influences SMC differentiation, migration and proliferation. Altogether, the present results suggest a potential direct pro-atherogenic role of PCSK9 in arterial SMCs.

Materials and Methods

Perivascular carotid collar placement

PCSK9 heterozygous were kindly provided by Dr. Philippe Costet (INSERM, Nantes) [20]. The colony was propagated by random intercrossing of heterozygous mutant mice to generate $PCSK9^{-/-}$ and $PCSK9^{+/+}$ mice. Littermates male mice with $PCSK9^{+/+}$ and $PCSK9^{-/-}$ genotypes were used in accordance with the Guide for the Care and Use of Laboratory Animals published by the US National Institutes of Health (NIH Publication No. 85-23, revised 1996). Mice were maintained on a normal diet (Mucedola, Milan, ITALY). Sixteen-week-old mice were anaesthetized by the intraperitoneal injection of Avertin (12 μl/gr body weight of 2.5% solution) and subjected to perivascular carotid collar placement. Collars (length: 3 mm, internal diameter: 0.38 mm, external diameter: 2.2 mm) were made from Tygon® tubing and were positioned around the right carotid artery. The contralateral left carotid artery was used as control. Following carotid injury, the animals were maintained on their dietetic regimens for 9 weeks, after which they were killed with an overdose of Avertin solution to harvest tissue specimens. Bloody samples were collected at sacrifice and analyzed by Fast Protein Liquid Chromatography (FPLC) analysis to identify the level of cholesterol in the lipoproteins (on a pool of 5 samples per group).

Histomorphometry

The collared segment of the right carotid artery and the corresponding segment of the contralateral sham-operated artery were collected at sacrifice and processed as previously described [19]. Briefly, tissue samples were fixed overnight in 4% paraformaldehyde, paraffin embedded, and cut transversally into 5 μm serial sections. One cross-section every 200 μm ≈ was stained with hematoxylin and eosin (H and E), photographed under a Zeiss Microscope mounted with a digital camera (Nikon Coolpix990) and morphometrically analyzed by using the OPTIMAS 6.2

image software (Media Cybernetics, Silverspring, MD). The cross-sectional areas of the intima and the media were measured directly and values were used to calculate the intima/media area ratio (*I*/*M*). The perimeters of the lumen and the external elastic lamina were recorded and used to derive the lumen area and the area surrounded by the external elastic lamina (EEL), respectively, using the formula perimeter $^{2} \cdot (4\pi)^{-1}$, to normalize for artifacts due to fixation or other steps of sample processing, including occasional deformation and potential tissue shrinkage.

Immunostaining and Picrosirius red staining

Immunostaining for cell type specific markers and Picrosirius red stain were performed on sections adjacent to those selected for morphometry. To detect α-smooth muscle actin (α-SMA)-positive vascular SMCs, sections were incubated with an anti α-SMA mouse polyclonal antibody (1:200, Biovision, Milpitas, CA). For detection of monocytes/macrophages, sections were blocked for endogenous peroxidase activity and for non-specific staining and incubated with F4/80 Rabbit mAb (1:100; Biovision); sections were then incubated with an avidin-biotin-peroxidase kit (ImmPRESS Reagent kit, Vector, Burlingame, CA) and visualized with 3,3-diaminobenzidine (Sigma-Aldrich, Milan), followed by hematoxylin counterstaining.

To detect intimal collagen, sections were stained with Picrosirius red (Direct red 80; Sigma-Aldrich) and analyzed under polarized light. Positive areas were determined by computer assisted image analysis (OPTIMAS 6.2), and related to total intimal surface area.

Cell culture reagents and antibodies for western blotting

Dulbecco's Modified Eagle Medium (DMEM), trypsin EDTA, penicillin, streptomycin, nonessential amino acid solution, and FBS were from Euroclone (Milan, ITALY). Plates and petri dishes were from Corning (Oneonta, New York). PDGF-BB was from Sigma-Aldrich. Molecular weight protein

standards, SDS, TEMED, ammonium persulfate, glycine, and acrylamide solution (30%T, 2.6%C) were obtained from BIO-RAD Laboratories (Hercules, CA). BCA assay for determination of protein concentrations was purchased from Thermo Fischer Scientific (Waltham, MA). For Western Blot analysis, the following antibodies were used: anti-PCSK9 (Cayman, Tallinn, Estonia), anti-α-tubulin (Sigma-Aldrich), anti-LDLR (Abcam, Cambridge, UK), and secondary IRDye800 Goat anti-mouse and anti-rabbit (Carlo Erba Reagents, Milan, ITALY).

Isolation and culture of mouse aortic SMCs

The murine aorta was cleaned from peripheral fat and adventitia. The aorta was dissected horizontally and smaller incisions were made longitudinally. The explants were kept in a six-well plate and subjected to mild heat fixation for 5-10 seconds. The explants were treated for one hour with a sterile solution of collagenases (type II, LS004171 Worthington Biochemical Corporation, NJ) to facilitate the migration of the SMCs from the vessel to the medium. The explants were supplemented with fresh DMEM High glucose (3 ml) containing 10% FCS. The presence of vascular SMCs was observed within one week. The cells were then trypsinised and plated for subsequent studies. For reducing the variability between cell strains, the explants were performed from a pool of 4 aortas of $PCSK9^{+/+}$ or $PCSK9^{-/-}$ mice.

RNA preparation and quantitative real-time PCR

Total RNA was extracted with the iScript Sample Preparation Buffer cDNA synthesis preparation reagents (BIO-RAD laboratories) according to manufacturer's instructions. Reverse transcription-polymerase first-strand cDNA synthesis was performed by using the Maxima 1^{st} strand DNA RT-qPCR (Thermo Fisher Scientific, Waltham, MA, USA). Quantitative real time PCR (qPCR) was then performed by using the Kit Thermo SYBR Green/ROX qPCR Master Mix (Thermo Fisher Scientific,

Waltham, MA, USA) and specific primers for selected genes. Primer sequences used for qPCR analysis are available upon request. The analyses were performed with the ABI Prism® 7000 Sequence Detection System (Applied Biosystems; Life Technologies Europe BV, Milan, ITALY). PCR cycling conditions were as follows: 94°C for 3min, 40 cycles at 94°C for 15s, and 60°C for 1min. Data were expressed as Ct values and used for the relative quantification of targets with the ΔΔCt calculation [21].

Western Blot Analysis

Cells were washed twice with PBS and lysed by incubation with a solution of 50 mM Tris pH 7.5, 150 mM NaCl, 0.5% Nonidet-P40, containing a protease and phosphatase inhibitor cocktails (Sigma-Aldrich) for 30 minutes on ice. Cell lysates were then cleared by centrifugation at 14,000 g for 10 minutes, and protein concentrations were determined using the BCA protein assay (Thermo Scientific, Rockford, IL). Equal amount of total protein per sample were separated by SDS-PAGE under reducing conditions, transferred to nitrocellulose membrane (GE Healthcare Little Chalfont, Buckinghamshire, UK) and subsequently immunoblotted with primary antibody following appropriate secondary fluorescently labeled antibody and acquired with the Odissey FC system (LI-COR, Nebraska). Quantitative densitometric analysis was performed with Image Studio software (LI-COR).

Generation of human PCSK9 expression constructs and retroviral infection

The retroviral expression plasmid encoding PCSK9-FLAG tag, was constructed using the pBM-IRES-PURO, expressing the puromycin resistance gene as a selectable second cistron gene, generated from the original pBM-IRES-EGFP, generously provided by G.P. Nolan (Stanford University, Stanford, CA). Human PCSK9-FLAG tag cDNA was kindly provided by Prof. P. Tarugi (University of Modena)

and subcloned into retroviral expression plasmid by blunt-end ligation.

Cell proliferation assay

SMCs were seeded in 24 well tray and incubated with DMEM supplemented with 10% FCS. Cell proliferation was evaluated by cell counting after trypsinization of the monolayers with use of a Coulter Counter model ZM at different time points. SMC doubling time was computed according to Elmore and Swift [22].

Cell migration assay

The Boyden chamber and the polycarbonate membrane were purchased from Biomap (Milan, Italy). The membranes were coated with a 0.1 mg/ml of type I collagen solution (PureCol®, Nutacon BV, Leimuiden, The Netherlands) in 0.1 M acetic acid at 37°C. The lower compartments of the wells of a modified Boyden chamber were filled (in triplicate) with DMEM containing 0.4% FCS in the absence or presence of PDGF-BB, whereas the upper compartments were filled with SMCs suspensions containing 10^6 cells/ml. The chamber was incubated at 37°C for 6 hours. The membrane was then carefully removed. Adherent SMCs on the top were eliminated and the membrane was stained with the Diff-Quik staining set (Biomap, Agrate Brianza, Milan Italy). The number of transmigrated cells was counted in four random high-power fields (HPFs) under high magnification (objective lens 20x).

Cytoskeleton staining

Cells were fixed in 4% paraformaldehyde at room temperature for 10 min, permeabilized in 0.1% Triton X-100 in phosphate-buffered saline for 15 min, and incubated with rhodamine-phalloidin (Sigma Aldrich, Milan, ITALY). Cytoskeleton staining of cells was analyzed using a fluorescence

microscope (Axiovert M220; Zeiss Instruments).

Real-time monitoring of cell morphology and cell proliferation using the iCELLigence system

The iCELLigence system (ACEA Biosciences Inc, San Diego CA, USA) monitors cellular events in realtime by recording the electrical impedance that is correlated with cell number, morphology and viability in a given culture well. For analyzing SMCs morphology, 40.000 cells/well were plated into the E-Plate L8, and the extent of cell spreading was monitored every 10 minutes for 6 hours with iCELLigence. For analyzing SMCs proliferation, instead, 10.000 cells/well were plated into the E-Plate L8, and their growth was monitored every hour for 5 days. The assay system expresses impedance in arbitrary Cell Index units (Rn-Rb)/4.6; where Rn is the cell-electrode impedance of the well when it contains cells and Rb is the background impedance of the well with the media alone.

G-LISA assay for Rac1 and RhoA

The intracellular amount of Rac1-GTP and RhoA-GTP were determined by using the G-LISA assay as previously described (Cytoskeleton, Inc Denver, CO, USA) [23-25].

Cell cycle analysis

Cells were trypsinised and centrifuged. The pellet of cells was washed with fresh PBS and re-centrifuged. The cells were re-suspended with the permeabilizing buffer (NaCl 100mM, TRIS pH 7.4 150mM; $CaCl_2$ 1mM; $MgCl_2$ 0.5mM; NP-40 0.1% containing 5 μM Propidium iodide). The analysis was performed by flow-cytometry by the use of a FACScan™ flow cytometer and analyzed with BD CellQuest™ (both from BD Biosciences, San Jose, CA).

Analysis of the data

Statistical analysis was performed using the Prism statistical analysis package version 6.0 (GraphPad Software, San Diego, CA). Data are given as mean ± SD of 3 independent experiments unless otherwise stated. P-values were determined by Student's t-test. A probability value of $p<0.05$ was considered statistically significant.

Results

Neointimal formation of PCSK9$^{+/+}$ and PCSK9$^{-/-}$ mice induced by carotid collar placement

To investigate the potential role of PCSK9 on SMC accumulation in the neointimal hyperplasia in response to vascular injury, we took advantage of the previously established "collar" model, based on the perivascular placement of a plastic cuff around the right common carotid artery [19]. Littermates sixteen-week-old PCSK9$^{-/-}$ and PCSK9$^{+/+}$ were subjected to perivascular carotid collar placement. Mice were fed normal chow diet for 9 weeks, after which they were sacrificed for the morphometric analysis of the right carotid specimens (n=14 animals per group). Representative microphotographs of collar-induced neointima formation are shown in Figure 1.

In both PCSK9$^{+/+}$ and $^{-/-}$ mice, collared carotid arteries showed the formation of intimal lesions that invaded the lumen region (Figure 1); in contrast, no neointimal formation was apparent in sham-operated carotid arteries and no morphological and anatomical differences were observed between the two strains (Figure 1). The determination of the morphological parameters showed a statistically significant reduction of neointimal formation, measured as intima area (23.955±1.832 μm^2 *vs* 12.344±1.668 μm^2 for PCSK9$^{+/+}$ and PCSK9$^{-/-}$ respectively; p=0.049) or intima/media ratio (1.380±0.175 *vs* 0.473±0.090; for PCSK9$^{+/+}$ and PCSK9$^{-/-}$ respectively; p=0.024), in PCSK9$^{-/-}$ mice, compared to PCSK9$^{+/+}$ (Figure 1B). These differences were associated to a tendency of a higher lumen area in PCSK9$^{-/-}$ mice (30.194±4.324 μm^2 *vs.* 18.283±1.912 μm^2), although it did not reach a statistical significance (Figure 1B). Determination of total cholesterol levels and lipoprotein distribution by FPLC analysis showed that at sacrifice mean serum total cholesterol was lower in PCSK9$^{-/-}$ than in PCSK9$^{+/+}$ mice (13.6 ± 3.3 mg/dL vs 47.1 ± 8.8 mg/dL; p<0.05) and mainly associated to HDL particles (Figure 1 C).

Immunostaining with anti α-smooth muscle actin (α-SMA) antibody showed that carotid lesions of PCSK9$^{+/+}$ mice had higher relative SMCs accumulation than PCSK9$^{-/-}$ (21.0±7.6% *vs.* 10.7±2.0% for PCSK9$^{+/+}$ and PCSK9$^{-/-}$ respectively; P<0.05) (Figure 2A). Analysis under polarized light of picrosirius red stained specimens, showed a higher relative collagen accumulation in PCSK9$^{+/+}$ mice (18.38±7.9% vs. 10.45±9.1% for PCSK9$^{+/+}$ and PCSK9$^{-/-}$ respectively; P<0.05) (Figure 2B), while no difference in macrophage content was detected, by immunostaining with anti F4/80 antibody, between the two groups (Figure 2C).

Determination of differentiation and proliferation of SMCs isolated from PCSK9$^{+/+}$ and PCSK9$^{-/-}$ mice

To further investigate the role of PCSK9 on neointimal hyperplasia, we isolated aortic SMCs from PCSK9$^{+/+}$ and PCSK9 $^{-/-}$ mice. As expected SMCs from PCSK9$^{-/-}$ mice did not express PCSK9, while western blot analysis clearly showed its expression in SMCs from PCSK9$^{+/+}$ animals. This difference was associated with increased levels of the LDLR in knock-out cells (Figure 3A). Different cell morphology was also observed between the two cell strains, with a spindle and elongated shape for PCSK9$^{-/-}$ SMCs and a more round morphology for the PCSK9$^{+/+}$ SMCs (Figure 3B). At passage one after isolation, the expression of phenotypic markers were determined by qPCR reaction under low serum condition (0.4% FCS). PCSK9$^{-/-}$ SMCs express higher levels of α-SMA (2.24±0.36 fold; P<0.01) and MHC-II (8.65±1.55 fold) and lower levels of caldesmon (-54±14%; P<0.01) (Figure 3C). In contrast, no differences were found on SM22α and calponin expression, while an almost significant reduction of Col1a1 mRNA levels were found in PCSK9$^{-/-}$ SMCs (-31±11%; P=0.06; Figure 3C) (Figure 3C).

Cell proliferation rate was then determined by cell counting experiments and iCelligence real time monitoring system (Figure 3D and 3E). Cell number after 3 and 6 days of stimulation with 10% FCS showed that PCSK9$^{-/-}$ SMCs have a lower proliferation rate than the PCSK9$^{+/+}$ (doubling

time equal to 57.3 ± 2.1 h vs 106.3 ± 4.5 h for PCSK9$^{+/+}$ and PCSK9$^{-/-}$, respectively) (Figure 3D). A similar difference was also observed by a real-time monitoring of cell growth with the iCelligence system, where PCSK9$^{-/-}$ SMCs appeared to slow down their proliferation rate after 60-70 h from the stimulation, while the PCSK9$^{+/+}$ SMCs continuously growth, up to 120 h after stimulation (Figure 3D).

The lower proliferation index of PCSK9$^{-/-}$ SMCs was also observed by analyzing the cell cycle progression from a quiescent (0.4% FCS) to a proliferative state in response to PDGF-BB (Figure 4A and 4B). In PCSK9$^{-/-}$ SMCs, 24h starvation with medium containing 0.4% FCS determined an accumulation of cells in the G0/G1 phase that was significantly higher than wild-type cells (76.1±0.5% vs. 69.1±0.6% for PCSK9$^{-/-}$ and PCSK9$^{+/+}$, respectively; $p<0.01$). Conversely, the stimulation with PDGF-BB determined a greater increase of cells in S phase in PCSK9$^{+/+}$ (from 9.8±0.5% to 14.8±0.1 %, Δ 5.0%) compared to PCSK9$^{-/-}$ SMCs (from 5.5±0.7% to 7.5±0.5%, Δ 2.0%).

Overall, the absence of PCSK9 appears to maintain SMCs in a more contractile phenotype, to reduce the expression of the major extracellular matrix protein (collagen type I) and to affect cell proliferation.

Reconstitution of PCSK9 in PCSK9$^{-/-}$ SMCs restores the proliferation and phenotypic behavior.

In order to better define the role of PCSK9 on SMCs biology, we took advantage of retroviral vectors, encoding for human PCSK9 FLAG tag, for stabling reconstitute the expression of PCSK9 in PCSK9$^{-/-}$ SMCs. Exogenous PCSK9 FLAG tag was detected in PCSK9 reconstituted cells (PCSK9 rec) by both using an antibody anti PCSK9 or an antibody anti FLAG, while it was not detectable in the control cells transduced with empty retroviral vector (Figure 5A and B). As expected, the expression of PCSK9 lowered the LDLR protein levels associated with a significant induction of LDLR mRNA levels (Figure 5C and D). Quantification of the SMC phenotypic markers by qPCR

analysis revealed that, by re-introducing the PCSK9 gene in the PCSK9$^{-/-}$ SMCs, the expression levels of α-SMA were reduced (-56±2%; P<0.01) while a significant induction of caldesmon was observed (1.46±0.3 fold; p<0.05; Figure 5E). On the contrary, no significant changes were seen for SM22α and Col1a1 (Figure 5E).

Reconstitution of PCSK9 by retroviral infection in PCSK9$^{-/-}$ SMCs determined a significant increase of cell proliferation rate, as assessed by both cell counting and real time monitoring with iCelligence system (Figure 5F and 5G).

Thus, the exogenous expression of PCSK9 in SMCs PCSK9$^{-/-}$ almost completely rescue the contractile phenotype of SMCs and induces a significant induction of cell proliferation. This evidence clearly demonstrates a pro-proliferative action of PCSK9 in primary SMCs.

Effect of PCSK9 on SMC migration

The determination of the migration capacity of PCSK9$^{+/+}$ and PCSK9$^{-/-}$ SMCs was then determined by using the Boyden's chamber chemotaxis assay with PDGF-BB as chemotactic agent. As shown in Figure 6A, compared to PCSK9$^{+/+}$ SMCs, PCSK9$^{-/-}$ SMCs expressed lower migratory capacity under both basal condition and after PDGF-BB stimulation.

The reconstitution of PCSK9 in PCSK9$^{-/-}$ SMCs (PCSK9 rec) determined an improvement of cell migration capacity both under basal condition and after stimulation with PDGF-BB (Figure 6B). These results clearly show that PCSK9 plays a direct role in modulating the migratory capacities of mouse SMCs.

Efficient cell migration requires a profound cytoskeleton re-organization and the formation protrusive structures termed lamellipodia, filopodia, invadopodia and podosomes [26]. Cytoskeletal staining with rhodamine-phalloidin showed that SMCs PCSK9$^{+/+}$ respond to PDGF-BB stimulation by acquiring an elongated morphology and by inducing lamellipodia formation (Figure 6C). On the

contrary, SMCs PCSK9$^{-/-}$ appear to be unresponsive to PDGF-BB, showing minor cytoskeletal changes in comparison to the basal condition (Figure 5C). The different morphological changes observed between the two cell lines were also investigated in real-time with the iCelligence system. As shown in Figure 6D, the cell index values did not change over time (up to 6 hours) under basal condition in both cell strains. However, the stimulation with PDGF-BB determined a profound increase of cell index values in SMCs PCSK9$^{+/+}$ with a maximal induction after approximately 1.5h and 2.5h, while in SMCs PCSK9$^{-/-}$ we observed a significant lower cell index values with a maximal pick after approximately 1.5h of stimulation (Figure 6D).

The determination of the intracellular amount of Rac1 and RhoA, in their active GTP-bound form by G-LISA assay, showed that in SMCs PCSK9$^{+/+}$ Rac1-GTP levels increased in response to PDGF-BB, while no effect was seen in SMCs PCSK9$^{-/-}$ (Figure 6E). As expected, PDGF-BB stimulation did not induce RhoA activity, however, it is interesting to note that the total amount of RhoA-GTP is significantly lower in SMCs PCSK9$^{-/-}$ in comparison to SMCs PCSK9$^{+/+}$ (Figure 6F).

Taken together, this evidence suggests that PCSK9 facilitates the response of SMCs to the chemotactic action of PDGF-BB, with the formation of lamellipodia protrusion and the activation of Rac1.

Discussion

In the present study, we have investigated a possible role of PCSK9 on vascular neointimal hyperplasia by using C57BL/6 wild type and PCSK9 knock out mice. The rationale of performing this analysis was mainly based on our previous observation that cultured SMCs expressed and secreted considerable amount of PCSK9 and that immunostaining with anti PCSK9 antibody revealed the presence of PCSK9 in human atherosclerotic plaques in regions occupied by α-actin positive cells [17].

The main finding of the study is that PCSK9 deficient mice are partially protected from the neointimal formation induced by periadventitial carotid placement of a non-occlusive collar. The morphometric analysis clearly shows that the difference between the $PCSK9^{+/+}$ and $PCSK9^{-/-}$ is almost exclusively related to the neointimal formation, with no changes in the area of the tunica media or in remodeling capacity. By immunohistochemical staining, it was shown that, in both groups of animal, the major cellular component of the neointima are smooth muscle α-actin positive cells while the macrophage component is minimal. In particular, compared to $PCSK9^{+/+}$, $PCSK9^{-/-}$ mice have a significantly lower percentage of the neointima occupied by SMCs. Conversely, no difference were found on macrophage content. Picrosirius red staining also showed that, in the absence of PCSK9, there was a lower deposition of fibrillary collagen in the neointima, an effect that was then confirmed by the observation that cultured $PCSK9^{-/-}$ SMCs express lower levels of collagen 1α1 mRNA.

A limitation of our study is that $PCSK9^{-/-}$ mice have significant lower plasma cholesterol levels compared to $PCSK9^{+/+}$, although in our experimental model neointimal hyperplasia is induced in normolipidemic mice. We have previously investigated the influence of hypercholesterolemia induced either by diet or genetic modification (apoE knock out mice), on neointima formation in the collar model, and clearly showed that cholesterol levels (from 78±14

mg/dL up to 1380 mg/dL) did not influence the size of the neointimal lesion but rather the plaque composition, with a higher inflammatory component and lipid deposition in hypercholesterolemic apoE knock out mice [19]. Thus, it is unlikely that the protective effect associated to the absence of PCSK9 observed in our study was driven by a lower levels of plasma cholesterol. In addition, we did not find any significant direct correlation between total plasma cholesterol level and intima/media values (data not shown).

The role of PCSK9 on atherosclerotic plaque development has been previously addressed by using transgenic and knock-out mice for PCSK9 fed hypercholesterolemic diet [27]. By crossing these mice with LDLR knock-out mice, Denis et al demonstrated that the incidence of PCSK9 on atherosclerotic plaque development was entirely dependent on the effect on LDLR and thus LDL cholesterol plasma levels [27]. On the contrary, the effect of PCSK9 on atherosclerosis appears to be independent of the regulation of cholesterol levels when the transgenic expression of PCSK9 was evaluated in apoE-deficient mice. In this model, PCSK9 overexpression determined a significant increase of atherosclerotic plaque without any significant alteration of cholesterol profile [27]. Thus, both our analysis and the study by Denis et al suggest a direct vascular effect of PCSK9.

As the neointimal hyperplasia is results from both migration and proliferation of SMCs, we further investigated the role of PCSK9 in cultured mouse SMCs isolated from $PCSK9^{+/+}$ and $PCSK9^{-/-}$ mice. The direct comparison of SMCs isolated by the two different mouse strains showed that freshly isolated $PCSK9^{-/-}$ SMCs expressed higher level of the contractile markers α-actin and MHC-II, and lower levels of the synthetic markers caldesmon and type I collagen. In addition, this cell strain showed a lower proliferative index and migratory capacity in comparison to $PCSK9^{+/+}$ SMCs. This data suggests that PCSK9 is likely to modulate both cell proliferation and migration as well as the switch from the contractile to the synthetic phenotype. This was then directly documented by reintroducing PCSK9 in $PCSK9^{-/-}$ cells. This system was employed in order to avoid strain-to-strain

differences between cell lines independent of PCSK9. The overexpression of PCSK9 showed an even greater positive effect on cell proliferation and migration accompanied by a significant modulation of α-SMA and caldesmon expression, further confirming the role of PCSK9 on SMCs.

The positive effect of PCSK9 on cell proliferation has been previously observed after partial hepatectomy in PCSK9$^{-/-}$ mice [28] and in hepatocyte cell line HepG2 following PCSK9 downregulation by shRNA [29]. Moreover, since in tumor cells the positive effect of PCSK9 on cell number is also associated with a reduction of apoptosis [29]. In our model, the relative contribution of lower proliferation versus higher apoptosis rate of SMCs on the less neointimal formation observed in PCSK9$^{-/-}$ remains to be determined.

The role of PCSK9 on cell migration has not been reported previously, although the effect of changes in cholesterol levels in the plasma membrane on cell adhesion and migration has been documented [30, 31]. In particular, the activity of Rac-1 and Rho-A is sensitive to cholesterol levels and distribution in the plasma membrane [32] and statins, by depleting the intracellular cholesterol, affects the invasive morphology of breast cancer cells [33]. Recruitment of integrins to focal adhesions and formation of focal adhesions at the leading edge of cells requires cholesterol [30, 34, 35] and the formation of specialized cholesterol-containing microdomains called caveolae [36]. Thus, it is tempting to speculate that the higher expression levels of LDLR, observed in SMCs PCSK9$^{-/-}$, could have been sufficient to alter the cholesterol membrane homeostasis and thus integrin recycling, focal adhesion formation, and lamellipodia protrusion to the leading edge of the cells and thus cell migration. In line with this hypothesis, we have observed an impairment of Rac1 activation and lamellipodia formation in response to PDGF-BB. However, more specific studies are required to define the role of PCSK9 on the caveolae formation and integrin recruitment to the cell membrane.

In conclusion, in the present study we provide evidence of a direct role of PCSK9 on neointimal formation in response to vascular injury whereby its absence determined an impairment of SMC proliferation and migration rate, potentially associated with the maintenance of a more contractile phenotype. These results unveil a pro-atherogenic role of PCSK9 that merits further investigations with the aim of highlighting potential direct benefits of PCSK9 inhibitors on atherogenesis and related vascular diseases beyond LDL cholesterol lowering.

Figure Legend

Figure 1. Histologic appearances and morphometric evaluation of collared and contralateral carotid arteries of PCSK9$^{+/+}$ and PCSK9$^{-/-}$ mice.

A) Representative hematoxylin and eosin staining of carotid cross-sections from PCSK9$^{+/+}$ and PCSK9$^{-/-}$ mice 9 weeks after collar placement. Control carotid arteries from both PCSK9$^{+/+}$ and PCSK9$^{-/-}$ mice did not show neointima formation. Bars = 100μm. B) Histograms showing the results of morphometric analysis. Intima/Media ratio was determined dividing the intimal area by the medial area. Lumen and EEL area were calculated using the formula perimeter^2 $(4\pi)^{-1}$. Data are expressed as mean±S.E. Differences between groups were assessed by Student's t-test, *p<0.05. C) FPLC analysis of plasma cholesterol profiles from PCSK9$^{+/+}$ and PCSK9$^{-/-}$ mice. The average cholesterol content of each FPLC fraction is shown.

Figure 2. Composition of collar-induced neointimal lesions of PCSK9$^{+/+}$ and PCSK9$^{-/-}$ mice.

A) Representative immunostaining with anti-α-SMA antibody (SMC marker) of cross-sections from collared carotids; quantification analysis is reported on the right histogram as percentage of α-SMA positive area in the intima. B) Representative staining with picrosirius red of fibrillary collagen visualized under polarized light; quantification analysis is reported on the right histogram as percentage of picrosirius red positive area in the intima. C) Representative immunostaining with anti-F4/80 (macrophage marker) antibody of cross-sections from collared carotids; quantification analysis is reported on the right histogram as percentage of F4/80 positive area in the intima. Data are expressed as mean±S.D. Differences between groups were assessed by Student's t-test, *p<0.05; **p<0.01.

Figure 3. Analysis of cell phenotype and proliferation rate of PCSK9$^{+/+}$ SMCs and PCSK9$^{-/-}$ SMCs.

A) PCSK9$^{+/+}$ SMCs and PCSK9$^{-/-}$ SMCs were seeded in DMEM/10% FCS and the day after starved for an additional 24h with DMEM containing 0.4% FCS. The protein expression of LDLR, PCSK9 and β-actin were then evaluated by western blot analysis. B) Morphology of PCSK9$^{+/+}$ SMCs and PCSK9$^{-/-}$ SMCs cultured with DMEM containing 10%FCS. C) Freshly isolated SMCs were cultured for 24h with DMEM containing 0.4% FCS. Total RNA was than extracted and smooth muscle markers expression levels evaluated by real time PCR. Differences between groups were assessed by Student's t-test, *P<0.05; **P<0.01. D) SMCs PCSK9$^{+/+}$ and PCSK9$^{-/-}$ were seeded at a density of $2{\cdot}10^4$/well (48 well tray) and incubated with DMEM supplemented with 10% FCS; 24h later the cells were counted with the Coulter Counter, after trypsinization of the monolayers (time 0). The same analysis was performed after 3 and 6 days. The cultured media were replaced every 3 days for maintaining a proper proliferation stimulus. Each bar represents the mean ± S.D. of triplicate dishes. For each time points, differences between groups were assessed by Student's t-test, ***P<0.001. E) Dynamic monitoring of cell proliferation was performed by using the iCelligence system. SMCs were cultured at time 0 at the density of $2{\cdot}10^4$/well (E-Plate L8) in DMEM containing 10%FCS, then the proliferation rate was monitored for 120h (5 days) every 15 minutes. Cell index is an adimentional value directly related to the cell number.

Figure 4. Cell cycle analysis of PCSK9$^{+/+}$ SMCs and PCSK9$^{-/-}$ SMCs in response to PDGF-BB.

Cells were seeded at a density of $2{\cdot}10^5$ in 35-mm dish and incubated with DMEM supplemented with 10% FCS. Twenty-four hours later, the medium was changed with medium containing 0.4% FCS to stop cell growth, and the cultures were incubated for 24h. At this time, PDGF-BB (20ng/ml) was added and cell cycle analysis performed after 24h. A) Representative flow cytometry analysis of PCSK9$^{+/+}$ SMCs and PCSK9$^{-/-}$ SMCs in the presence or absence of PDGF-BB. B) Percentage of cells

in the different cell cycle phases. The percentage of cells in S phase of $PCSK9^{+/+}$ SMCs and $PCSK9^{-/-}$ SMCs after stimulation with PDGF-BB was statistically significant as assessed by Student's t-test, P=0.01.

Figure 5. Analysis of phenotype and proliferation rate after PCSK9 reconstitution of SMCs $PCSK9^{-/-}$. SMCs $PCSK9^{-/-}$ were retrovirally transduced with empty retroviral vector or encoding for human PCSK9 FLAG-tag. After puromycin selection, the expression of PCSK9 was evaluated by western blot analysis from total cell lysates using an anti-PCSK9 antibody (A) or anti-FLAG antibody (B). LDLR expression was evaluated by Western blot analysis (C) or quantitative real time PCR (D). E) SMCs were cultured for 24h with DMEM containing 0.4% FCS. Total RNA was than extracted and smooth muscle markers expression levels evaluated by real time PCR. Differences between groups were assessed by Student's t-test, *P<0.05; **P<0.01. F) SMCs were seeded at a density of $2 \cdot 10^4$/well (48 well tray) and incubated with DMEM supplemented with 10% FCS; 24 h later the cells were counted with the Coulter Counter, after trypsinization of the monolayers (time 0). The same analysis was performed after 3 and 6 days. The cultured media were replaced every 3 days for maintaining a proper proliferation stimulus. Each bar represents the mean ± S.D. of triplicate dishes. For each time points, differences between groups were assessed by Student's t-test, ***P<0.001. G) Dynamic monitoring of cell proliferation was performed by using the iCelligence system. SMCs were cultured at time 0 at the density of $2 \cdot 10^4$/well (E-Plate L8) in DMEM containing 10% FCS, then the proliferation rate was monitored for 120 h (5 days) every 15 minutes. Cell index is an adimentional value directly related to the cell number. Rec. stays for $PCSK9^{-/-}$ SMCs expressing human PCSK9 FLAG-tag after retroviral infection and puromycin selection, -/- stays for $PCSK9^{-/-}$ SMCs retrovirally infected with empty control vector containing the puromycin resistant gene.

Figure 6. Effect of PCSK9 on SMCs migration in response to PDGF-BB.

A) $PCSK9^{+/+}$ SMCs and $PCSK9^{-/-}$ SMCs were cultured for 24h in DMEM containing 0.4% FCS. After 24h, cells were harvested by trypsinization and the migration measured by Boyden's chamber chemotactic assay by using PDGF-BB as chemotactic agent at the indicated concentrations. Transmigrated cells were counted in four random high-power fields (HPFs) under high magnification (objective lens 20×). Basal indicates cells incubated in DMEM/0.4% FCS without PDGF-BB; Differences between groups were assessed by Student's t-test, *P<0.05; **P<0.01. B). The same analysis described in panel A was performed with $PCSK9^{-/-}$ SMCs and PCSK9 rec SMCs. Differences between groups were assessed by Student's t-test, **P<0.01; ***P<0.001. C) Cytoskeletal organization of SMCs were analyzed under basal condition (DMEM/0.4% FCS) or 15 min. stimulation with PDGF-BB (20 ng/ml). F-actin is stained red with rhodamine-phalloidin while nuclei are stained blue with DAPI. D) Morphological changes in $PCSK9^{-/-}$ SMCs and $PCSK9^{+/+}$ SMCs were recorded by iCelligence system under basal condition (DMEM/0.4% FCS) and after stimulation with PDGF-BB for 6h. E and F). Intracellular levels of Rac-1-GTP and RhoA-GTP levels were determined by G-LISA assay under basal condition (DMEM/0.4% FCS) and after stimulation for 5 min. with 20 ng/ml of PDGF-BB.

Acknowledgements

This wok was supported by Fondazione Cariplo grant Rif. 2012-0549

References

1) Ross R: The pathogenesis of atherosclerosis: a perspective for the 1990s. Nature, 1993; 362:801-809.

2) Raines EW and Ferri N: Thematic review series: The immune system and atherogenesis. Cytokines affecting endothelial and smooth muscle cells in vascular disease. J Lipid Res, 2005; 46:1081-1092

3) Doran AC, Meller N and McNamara CA: Role of smooth muscle cells in the initiation and early progression of atherosclerosis. Arterioscler Thromb Vasc Biol, 2008; 28:812-819

4) Campbell JH and Campbell GR: The role of smooth muscle cells in atherosclerosis. Curr Opin Lipidol, 1994; 5:323-330

5) Worth NF, Rolfe BE, Song J and Campbell GR: Vascular smooth muscle cell phenotypic modulation in culture is associated with reorganisation of contractile and cytoskeletal proteins. Cell motility and the cytoskeleton, 2001; 49:130-145

6) Raines EW, Koyama H and Carragher NO: The extracellular matrix dynamically regulates smooth muscle cell responsiveness to PDGF. Annals of the New York Academy of Sciences, 2000; 902:39-51; discussion 51-32

7) Corjay MH, Thompson MM, Lynch KR and Owens GK: Differential effect of platelet-derived growth factor- versus serum-induced growth on smooth muscle alpha-actin and nonmuscle beta-actin mRNA expression in cultured rat aortic smooth muscle cells. J Biol Chem, 1989; 264:10501-10506

8) Reusch P, Wagdy H, Reusch R, Wilson E and Ives HE: Mechanical strain increases smooth muscle and decreases nonmuscle myosin expression in rat vascular smooth muscle cells. Circ Res, 1996; 79:1046-1053

9) Su B, Mitra S, Gregg H, Flavahan S, Chotani MA, Clark KR, Goldschmidt-Clermont PJ and Flavahan NA: Redox regulation of vascular smooth muscle cell differentiation. Circ Res, 2001; 89:39-46

10) Pidkovka NA, Cherepanova OA, Yoshida T, Alexander MR, Deaton RA, Thomas JA, Leitinger N and Owens GK: Oxidized phospholipids induce phenotypic switching of vascular smooth muscle cells in vivo and in vitro. Circ Res, 2007; 101:792-801

11) Ang AH, Tachas G, Campbell JH, Bateman JF and Campbell GR: Collagen synthesis by cultured rabbit aortic smooth-muscle cells. Alteration with phenotype. Biochem J, 1990; 265:461-469

12) Dusserre E, Bourdillon MC, Ciavatti M, Covacho C and Renaud S: Lipid biosynthesis in cultured arterial smooth muscle cells is related to their phenotype. Lipids, 1993; 28:589-592

13) Campbell JH, Popadynec L, Nestel PJ and Campbell GR: Lipid accumulation in arterial smooth muscle cells. Influence of phenotype. Atherosclerosis, 1983; 47:279-295

14) Robinson JG, Farnier M, Krempf M, Bergeron J, Luc G, Averna M, Stroes ES, Langslet G, Raal FJ, El Shahawy M, Koren MJ, Lepor NE, Lorenzato C, Pordy R, Chaudhari U, Kastelein JJ and Investigators OLT: Efficacy and safety of alirocumab in reducing lipids and cardiovascular events. N Engl J Med, 2015; 372:1489-1499

15) Sabatine MS, Giugliano RP, Wiviott SD, Raal FJ, Blom DJ, Robinson J, Ballantyne CM, Somaratne R, Legg J, Wasserman SM, Scott R, Koren MJ, Stein EA and Open-Label Study of Long-Term Evaluation against LDLCI: Efficacy and safety of evolocumab in reducing lipids and cardiovascular events. N Engl J Med, 2015; 372:1500-1509

16) Seidah NG, Benjannet S, Wickham L, Marcinkiewicz J, Jasmin SB, Stifani S, Basak A, Prat A and Chretien M: The secretory proprotein convertase neural apoptosis-regulated

convertase 1 (NARC-1): liver regeneration and neuronal differentiation. Proc Natl Acad Sci U S A, 2003; 100:928-933

17) Ferri N, Tibolla G, Pirillo A, Cipollone F, Mezzetti A, Pacia S, Corsini A and Catapano AL: Proprotein convertase subtilisin kexin type 9 (PCSK9) secreted by cultured smooth muscle cells reduces macrophages LDLR levels. Atherosclerosis, 2012; 220:381-386

18) Perisic L, Hedin E, Razuvaev A, Lengquist M, Osterholm C, Folkersen L, Gillgren P, Paulsson-Berne G, Ponten F, Odeberg J and Hedin U: Profiling of atherosclerotic lesions by gene and tissue microarrays reveals PCSK6 as a novel protease in unstable carotid atherosclerosis. Arterioscler Thromb Vasc Biol, 2013; 33:2432-2443

19) Baetta R, Silva F, Comparato C, Uzzo M, Eberini I, Bellosta S, Donetti E and Corsini A: Perivascular carotid collar placement induces neointima formation and outward arterial remodeling in mice independent of apolipoprotein E deficiency or Western-type diet feeding. Atherosclerosis, 2007; 195:e112-124

20) Le May C, Kourimate S, Langhi C, Chetiveaux M, Jarry A, Comera C, Collet X, Kuipers F, Krempf M, Cariou B and Costet P: Proprotein convertase subtilisin kexin type 9 null mice are protected from postprandial triglyceridemia. Arterioscler Thromb Vasc Biol, 2009; 29:684-690

21) Ferri N, Colombo G, Ferrandi C, Raines EW, Levkau B and Corsini A: Simvastatin reduces MMP1 expression in human smooth muscle cells cultured on polymerized collagen by inhibiting Rac1 activation. Arterioscler Thromb Vasc Biol, 2007; 27:1043-1049

22) Elmore E and Swift M: Growth of cultured cells from patients with ataxia-telangiectasia. Journal of cellular physiology, 1976; 89:429-431

23) Ferri N, Bernini SK, Corsini A, Clerici F, Erba E, Stragliotto S and Contini A: 3-Aryl-N-aminoylsulfonylphenyl-1H-pyrazole-5-carboxamides: a new class of selective Rac inhibitors. Medchemcomm, 2013; 4:537-541

24) Ferri N, Corsini A, Bottino P, Clerici F and Contini A: Virtual screening approach for the identification of new Rac1 inhibitors. Journal of medicinal chemistry, 2009; 52:4087-4090

25) Ruffoni A, Ferri N, Bernini SK, Ricci C, Corsini A, Maffucci I, Clerici F and Contini A: 2-Amino-3-(phenylsulfanyl)norbornane-2-carboxylate: An Appealing Scaffold for the Design of Rac1-Tiam1 Protein-Protein Interaction Inhibitors. Journal of medicinal chemistry, 2014;

26) Buccione R, Orth JD and McNiven MA: Foot and mouth: podosomes, invadopodia and circular dorsal ruffles. Nature reviews Molecular cell biology, 2004; 5:647-657

27) Denis M, Marcinkiewicz J, Zaid A, Gauthier D, Poirier S, Lazure C, Seidah NG and Prat A: Gene inactivation of proprotein convertase subtilisin/kexin type 9 reduces atherosclerosis in mice. Circulation, 2012; 125:894-901

28) Zaid A, Roubtsova A, Essalmani R, Marcinkiewicz J, Chamberland A, Hamelin J, Tremblay M, Jacques H, Jin W, Davignon J, Seidah NG and Prat A: Proprotein convertase subtilisin/kexin type 9 (PCSK9): hepatocyte-specific low-density lipoprotein receptor degradation and critical role in mouse liver regeneration. Hepatology, 2008; 48:646-654

29) Sun X, Essalmani R, Day R, Khatib AM, Seidah NG and Prat A: Proprotein convertase subtilisin/kexin type 9 deficiency reduces melanoma metastasis in liver. Neoplasia, 2012; 14:1122-1131

30) Ramprasad OG, Srinivas G, Rao KS, Joshi P, Thiery JP, Dufour S and Pande G: Changes in cholesterol levels in the plasma membrane modulate cell signaling and regulate cell adhesion and migration on fibronectin. Cell motility and the cytoskeleton, 2007; 64:199-216

31) Hoque M, Rentero C, Conway JR, Murray RZ, Timpson P, Enrich C and Grewal T: The cross-talk of LDL-cholesterol with cell motility: insights from the Niemann Pick Type C1 mutation and altered integrin trafficking. Cell adhesion & migration, 2015; 9:384-391

32) Navarro-Lerida I, Sanchez-Perales S, Calvo M, Rentero C, Zheng Y, Enrich C and Del Pozo MA: A palmitoylation switch mechanism regulates Rac1 function and membrane organization. The EMBO journal, 2012; 31:534-551

33) Freed-Pastor WA, Mizuno H, Zhao X, Langerod A, Moon SH, Rodriguez-Barrueco R, Barsotti A, Chicas A, Li W, Polotskaia A, Bissell MJ, Osborne TF, Tian B, Lowe SW, Silva JM, Borresen-Dale AL, Levine AJ, Bargonetti J and Prives C: Mutant p53 disrupts mammary tissue architecture via the mevalonate pathway. Cell, 2012; 148:244-258

34) Kanerva K, Uronen RL, Blom T, Li S, Bittman R, Lappalainen P, Peranen J, Raposo G and Ikonen E: LDL cholesterol recycles to the plasma membrane via a Rab8a-Myosin5b-actin-dependent membrane transport route. Developmental cell, 2013; 27:249-262

35) Garcia-Melero A, Reverter M, Hoque M, Meneses-Salas E, Koese M, Conway JR, Johnsen CH, Alvarez-Guaita A, Morales-Paytuvi F, Elmaghrabi YA, Pol A, Tebar F, Murray RZ, Timpson P, Enrich C, Grewal T and Rentero C: Annexin A6 and Late Endosomal Cholesterol Modulate Integrin Recycling and Cell Migration. J Biol Chem, 2016; 291:1320-1335

36) Echarri A and Del Pozo MA: Caveolae internalization regulates integrin-dependent signaling pathways. Cell cycle, 2006; 5:2179-2182

***Statement of Originality**

UNIVERSITÀ
DEGLI STUDI
DI PADOVA

Dr. Arnold von Eckardstein

Editor-in-Chief of Atherosclerosis

February 29th 2016

Dear Dr. von Eckardstein

Please find enclosed our manuscript "PCSK9 knock out mice are protected from neointimal formation in response to perivascular carotid collar placement" by Nicola Ferri et al that would like to submit to "Atherosclerosis" for consideration as Research Paper.

The contents of this manuscript have not been previously published and are not currently submitted elsewhere. All authors are in agreement with submission of the manuscript to Atherosclerosis.

Sincerely yours,

Dr. Nicola Ferri

UNIVERSITÀ DEGLI STUDI DI PADOVA

Dr. Arnold von Eckardstein

Editor-in-Chief of Atherosclerosis

February 29th 2016

Dear Dr. von Eckardstein

Please find enclosed our manuscript "PCSK9 knock out mice are protected from neointimal formation in response to perivascular carotid collar placement" by Nicola Ferri et al that would like to submit to "Atherosclerosis" for consideration as Research Paper.

In this study, we have provided an original observation that PCSK9 knockout mice developed less neointimal formation in response to perivascular manipulation. The carotid manipulation was induced by periadventitial placement of a non-occlusive collar in PCSK9 knockout (PCSK9-/-) and wild type (WT) littermate (PCSK9+/+) mice fed normal chow diet. After 9 weeks of vascular injury, we have observed a significant reduction of neointimal formation and less accumulation of smooth muscle cells (SMCs) in the lesions. This *in vivo* effect is potentially the result of an impairment of PCSK9-/- mSMCs on proliferation, differentiation and migration process. Indeed, cultured PCSK9-/- mSMCs proliferation and migration rates were lower than wild-type cells. In addition, the reconstitution of PCSK9 in PCSK9-/- mSMCs rescues the proliferation and the migration capacity of PCSK9-/- mSMCs.

Taken together, the present study suggest an atherogenic role of PCSK9 through the sustainment of SMC synthetic phenotype, proliferation and migration. This evidence may have a clinical impact and significance for a potential anti-restenosis effect of monoclonal antibodies anti PCSK9, currently utilized in animal studies.

Suggested reviewers:

Bodo Levkau e-mail: levkau@uni-essen.de

Elaine W. Raines e-mail: ewraines@u.washington.edu

Bertrand Cariou e-mail: bertrand.cariou@univ-nantes.fr

Paolo Parini e-mail: paolo.parini@ki.se

We look forward to the manuscript's review

Sincerely yours,

Dr. Nicola Ferri

***Conflict of interest form**

UNIVERSITÀ DEGLI STUDI DI PADOVA

Dr. Arnold von Eckardstein

Editor-in-Chief of Atherosclerosis

February 29th 2016

Dear Dr. von Eckardstein

All the authors declare that they have no conflicts of interest with the contents of this article.

Sincerely yours,

Dr. Nicola Ferri

Figure 1

Click here to download high resolution image

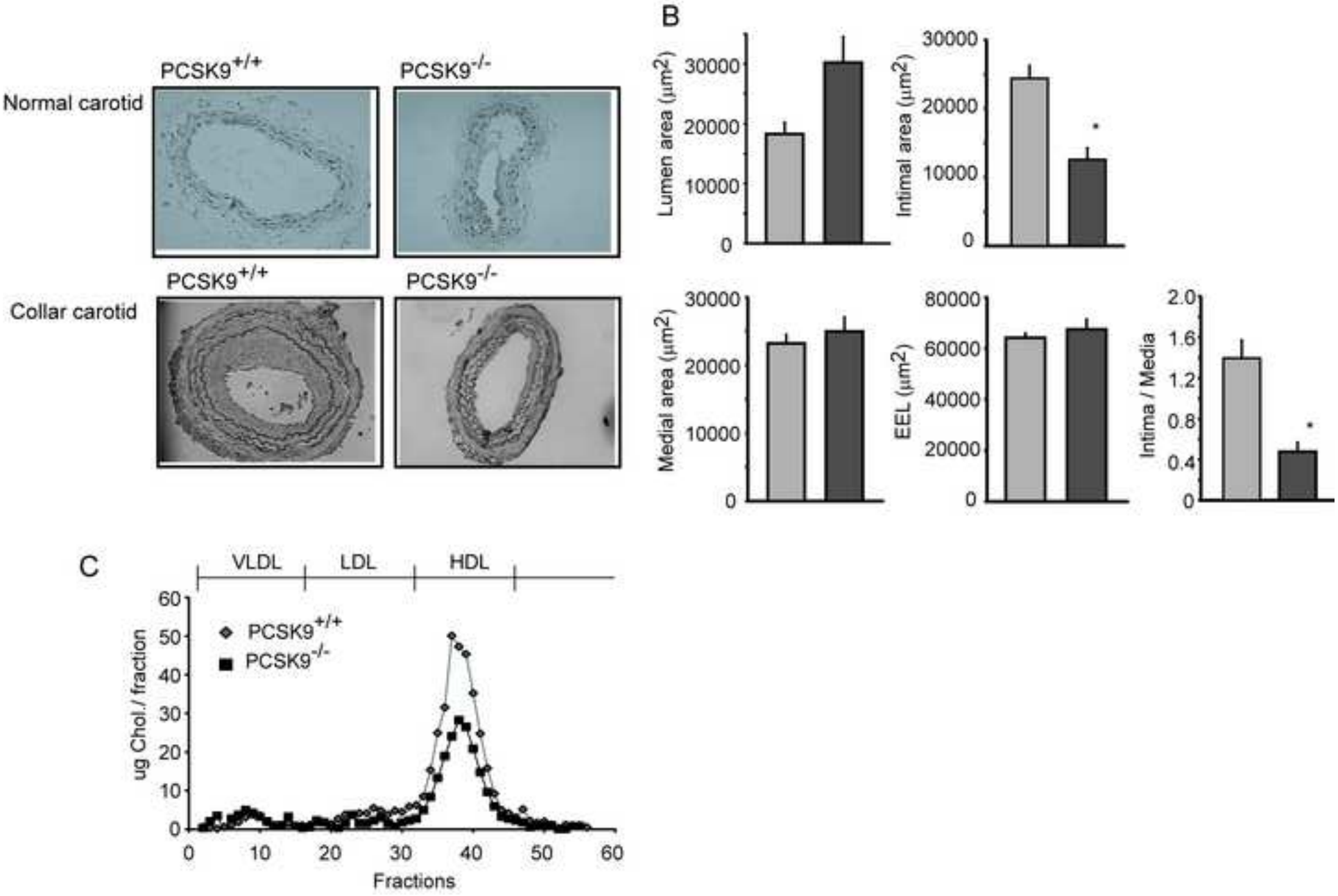

Figure 2

Click here to download high resolution image

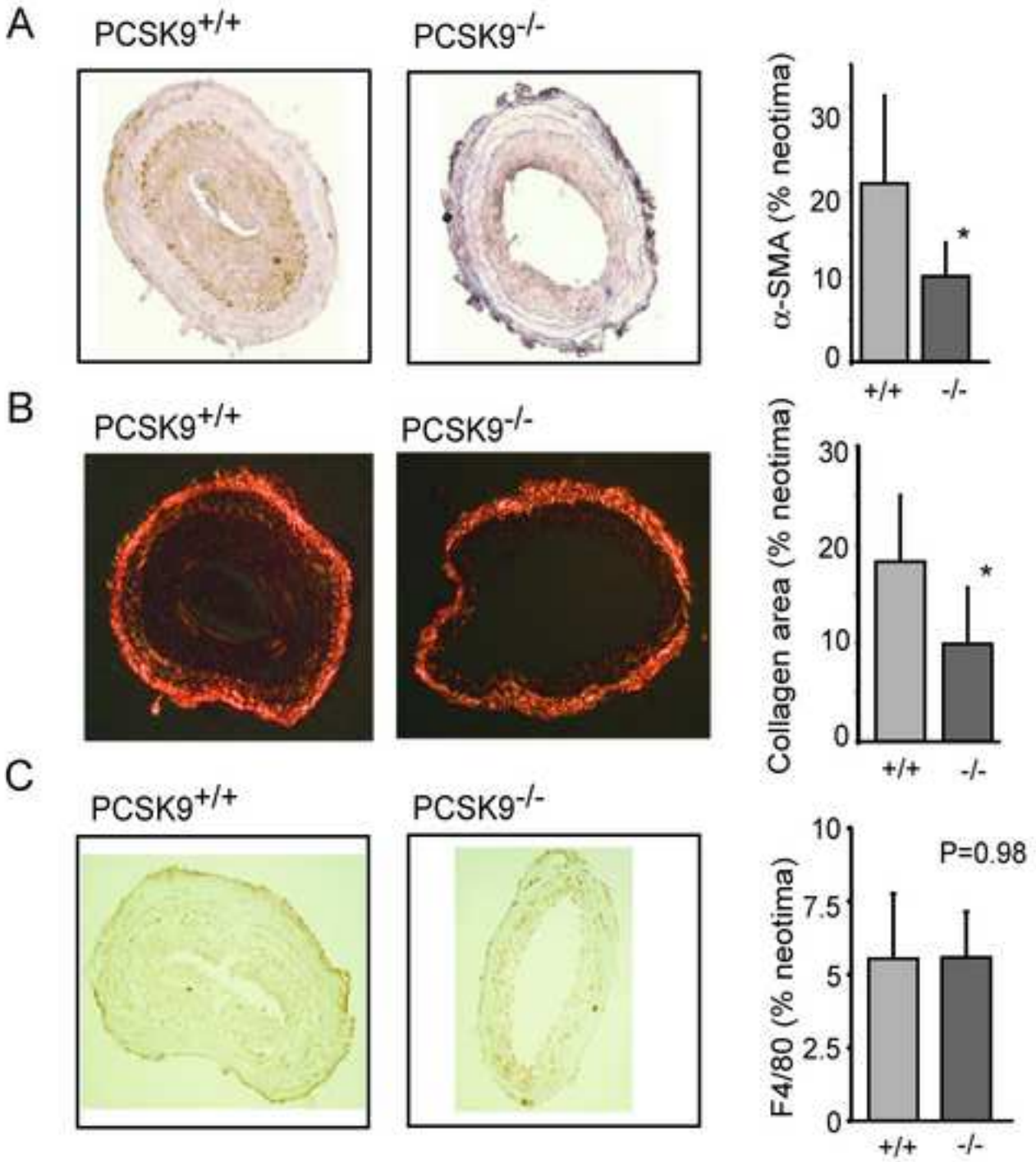

Figure 2

Click here to download high resolution image

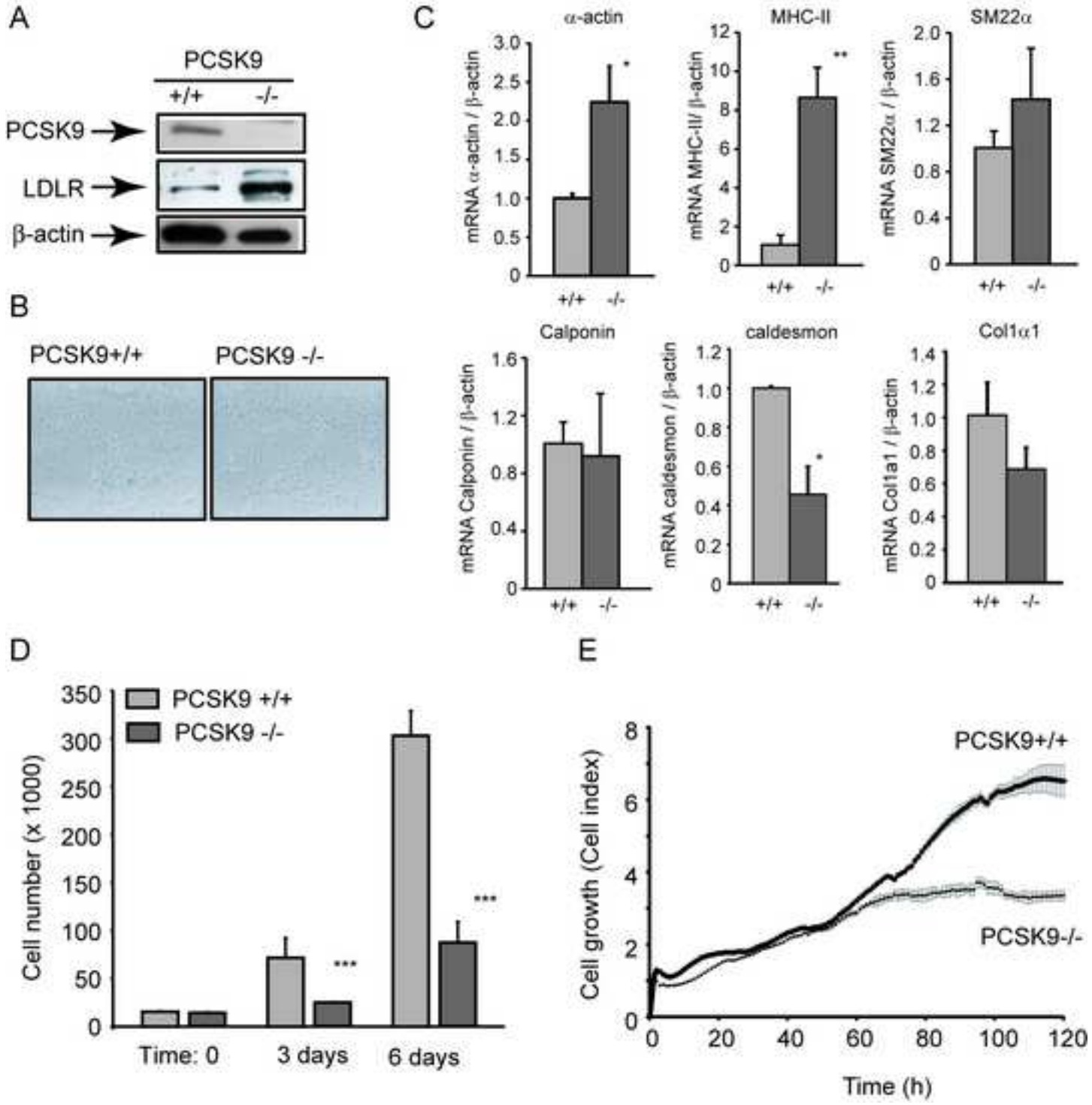

Figure 4

Click here to download high resolution image

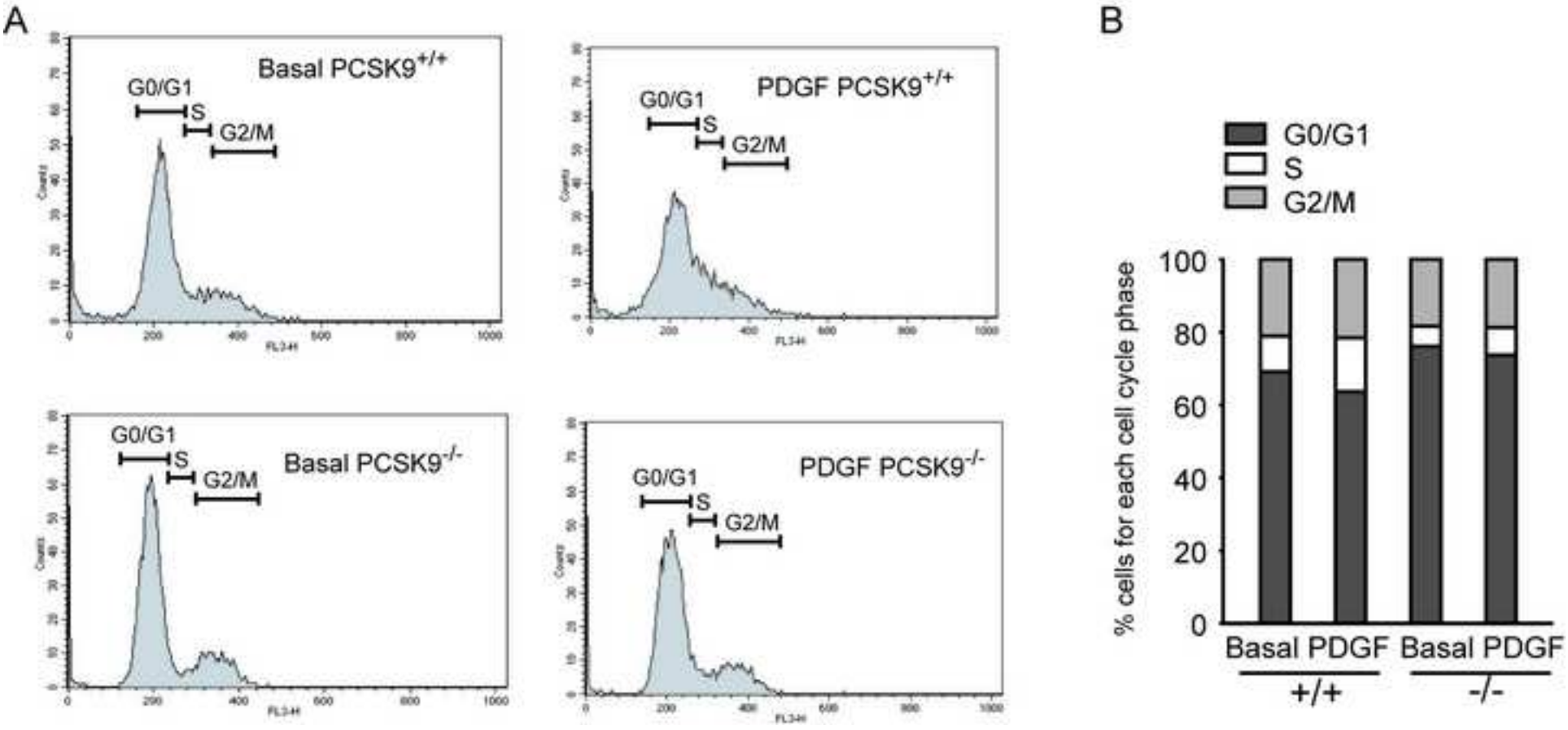

Figure 5

Click here to download high resolution image

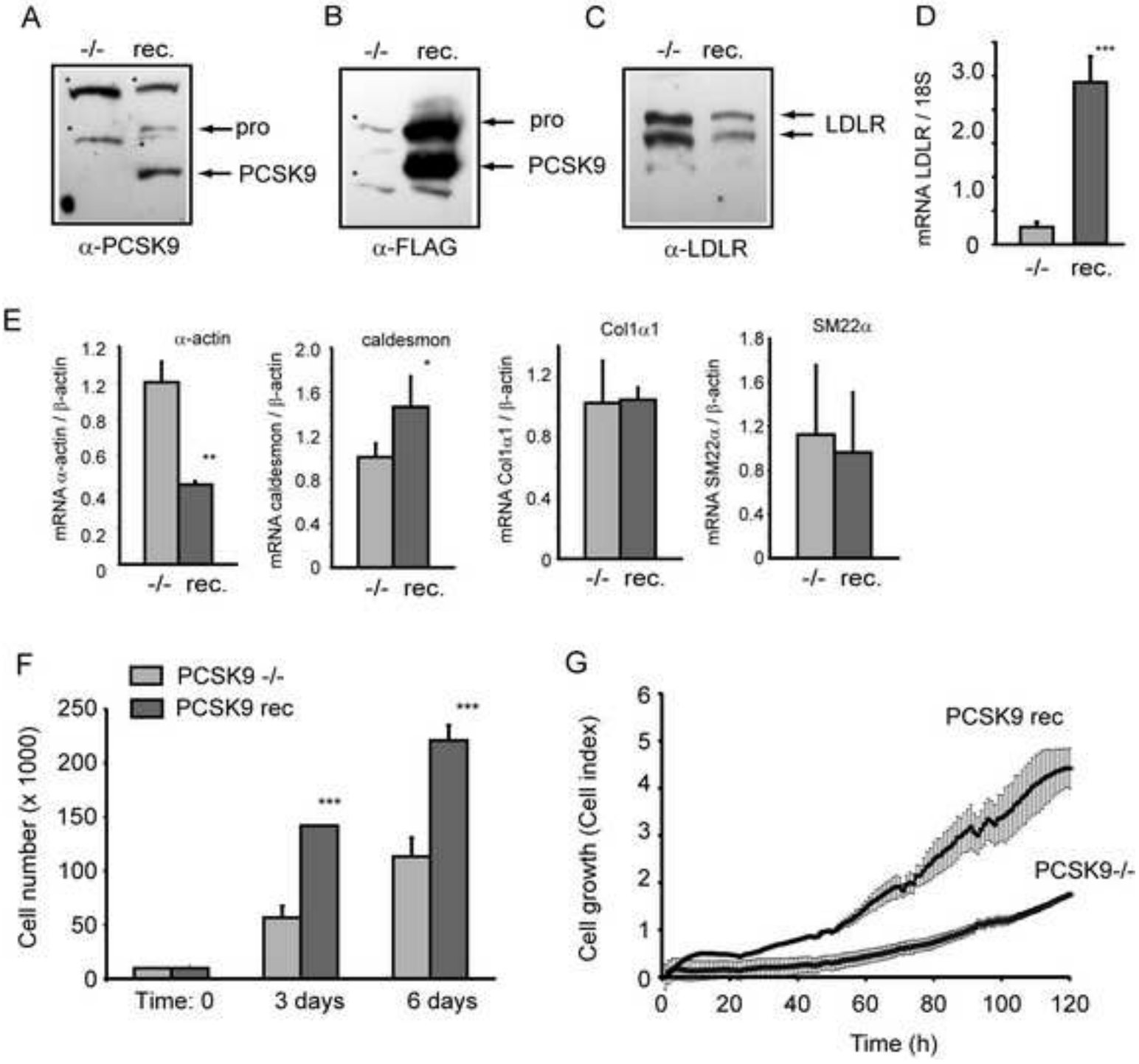

Figure 6

Click here to download high resolution image